International Journal of Heat and Mass Transfer 52 (2009) 4757–4765

Contents lists available at ScienceDirect

International Journal of Heat and Mass Transfer

journal homepage: www.elsevier.com/locate/ijhmt

Analytic modelling of a falling film absorber and experimental determination of transfer coefficients

D.S. Kim [a,*], C.A. Infante Ferreira [b,1]

[a] Arsenal Research, Sustainable Energy Systems, Giefinggasse 2, 1210 Vienna, Austria
[b] Delft University of Technology, Engineering Thermodynamics, Leeghwaterstraat 44, 2628 CA Delft, The Netherlands

ARTICLE INFO

Article history:
Received 4 April 2007
Received in revised form 15 April 2009
Available online 20 July 2009

Keywords:
Analytic model
Falling film flow
Absorption
Transfer coefficient
LiBr

ABSTRACT

Accurate interpretation of the experimental data on falling film flows is a critical part of the investigations in the field of absorption energy system research. However, there is no theoretically proven way to determine experimental heat and mass transfer coefficients for non-isothermal absorption falling film flows. In this article, firstly, it is shown how the governing equations of a falling film absorber can be reduced to two ordinary differential equations and analytic expressions can be obtained for the temperature and concentration profiles along the absorber. Secondly, a new method is proposed to determine heat and mass transfer coefficients from experimental data and its application is demonstrated by reprocessing the experimental data from two experimental studies reported in the literature. The results show that some of the experimental data were misinterpreted by conventional methods and the errors were negligible only when heat and mass fluxes were small, which agrees with the fact that the obtained analytic solutions approach the conventional logarithmic heat and mass transfer equations in such conditions.

1. Introduction

In contrast with single-phase heat transfer or isothermal absorption, significant changes both in composition and temperature accompany the sorption processes in absorption refrigeration systems. The complexity of physical mechanisms in the non-isothermal sorption processes has been forcing researchers to resort mostly on experiments. However, there has been a great confusion in the interpretation of experimental data regarding the true driving potentials in the heat and mass transfer processes. Various definitions of heat and mass transfer coefficients can be found in the literature and to make matters worse, most of them lack theoretical basis. The invalidity of conventional methods has been recently investigated by Islam et al. [1–3] and Fujita and Hihara [4] and some alternative methods have been proposed. However, these alternatives have some weaknesses, which will be pointed out at the end of this section, and the problem remains largely unsolved.

First of all, various definitions of heat and mass transfer coefficients found in the literature are briefly discussed in the following (see Fig. 1 for notations).

Wall heat flux is commonly defined by

$$\dot{q}^w = k\left(\frac{\partial T}{\partial y}\right)_{y=0} \equiv \alpha'(T - T^w) \tag{1}$$

where T^w is the wall temperature, T is the solution temperature and α' is a local heat transfer coefficient. In the literature, different solution temperatures have been chosen for T including bulk solution temperature T^b, equilibrium solution temperature T^s and interface temperature T^i.

The heat rejection to the cooling water can be written as

$$\dot{q}^w_{avg} = U\Delta T_{avg} \tag{2}$$

where U is an overall heat transfer coefficient and ΔT_{avg} is an average temperature difference most commonly defined as

$$\Delta T_{avg} \equiv \frac{(T-t)_{top} - (T-t)_{bot}}{\ln[(T-t)_{top}/(T-t)_{bot}]} \tag{3}$$

Many studies [5–8] used T^b for T in Eqs. (1)–(3). On the other hand, [9–11] used equilibrium bulk solution temperatures calculated from bulk concentration and pressure, i.e. $T^s(x^b,p)$, and [12] used T^i calculated from T^b and x^b using the model of Yüksel and Schlünder [13]. Takamatsu et al. [14] measured local wall temperatures and calculated average heat transfer coefficients with the arithmetic averages of T^b and T^w.

Rather unusually, Miller and Keyhani [15] used $\Delta T_{avg} = T^i_{top} - t_{bot}$, which is the maximum temperature difference in the

* Corresponding author. Tel.: +43 505506668; fax: +43 505506613.
E-mail addresses: dong-seon.kim@arsenal.ac.at (D.S. Kim), C.A.InfanteFerreira@tudelft.nl (C.A. Infante Ferreira).
[1] Tel.: +31 152784894.

0017-9310/$ - see front matter © 2009 Elsevier Ltd. All rights reserved.
doi:10.1016/j.ijheatmasstransfer.2009.05.014

Nomenclature

A	area, m^2
a	constant in Eq. (A.4)
B	constant in Eq. (18)
b, c	constant in Eq. (B.4)
C	constant in Eq. (17)
Cp	heat capacity, kJ kg^{-1} K^{-1}
c_{1-3}	constants in Eq. (13)
D	mass diffusivity, m^2 s^{-1}
F	constant in Eq. (B.6)
g	gravity constant, m s^{-2}
h	specific enthalpy, kJ kg^{-1}
h^{fg}	latent heat, kJ kg^{-1}
$\bar{h}$	partial specific enthalpy, kJ kg^{-1} of a species
k	thermal conductivity, kW m^{-1} K^{-1}
L	absorber length, m
Le	Lewis number, $(k/\rho Cp)/D$
Nu	Nusselt number, $\alpha^b/k \times (\nu^2/g)^{1/3}$
n	exponent of Lewis number in Eq. (B.10)
$\dot{n}$	mass flux, kg m^{-2} s^{-1}
p	pressure, kPa
$\dot{q}$	heat flux, kW m^{-2}
Re_f	film Reynolds number, $4\Gamma_s/\mu$
s	distance along vapour-liquid interface, m
Sh	Sherwood number, $\beta/D \times (\nu^2/g)^{1/3}$
St_h	Stanton number for interface heat transfer, $\alpha^i/\dot{n}Cp_w$
St_m	Stanton number for mass transfer, $\rho\beta/\dot{n}$
T	temperature of solution or vapour, K
t	temperature of cooling water, K
U	average overall heat transfer coefficient, kW m^{-2} K^{-1}
u	velocity in z direction, m s^{-1}
$\overline{U}$	dimensionless heat transfer coefficient, $UL/\Gamma_s Cp_s$
$v_{1,2}$	eigenvector components
x	mass fraction of absorbent in solution
y	distance perpendicular to flow direction, m
z	distance in flow direction, m

Greek symbols

α'	local heat transfer coefficient, kW m^{-2} K^{-1}
α	average heat transfer coefficient, kW m^{-2} K^{-1}
β'	local mass transfer coefficient, m s^{-1}
β	average mass transfer coefficient, m s^{-1}
$\bar{\beta}$	dimensionless mass transfer coefficient, $\rho\beta L/\Gamma_s$
Γ	mass flow per unit perimeter, kg m^{-1} s^{-1}
Δh	heat of absorption ($\Delta h = a h^{fg}$), kJ kg^{-1}
ΔT	temperature difference, K
Δ_T	thermal boundary layer thickness at the interface, m
Δx	concentration difference or driving potential for mass transfer
Δ_x	concentration boundary layer thickness at the interface, m
δ	film thickness, m
ζ	dimensionless distance in flow direction, z/L
$\lambda_{1,2}$	eigenvalues
μ	dynamic viscosity, Pa s
ν	kinematic viscosity, m^2 s^{-1}
ρ	density, kg m^{-3}
Φ_h	correction factor for interface heat transfer in Eq. (B.8)
φ	dimensionless thermal mass flux, $\dot{n}Cp_w/\alpha^i$
Φ_m	correction factor for mass transfer in Eq. (B.2)
ϕ	dimensionless mass flux or driving potential for mass transfer, $\dot{n}/\rho\beta(= x^b - x^i)$
ω	dimensionless wall heat flux, $\dot{q}^w Cp_s/U\Delta h[= (T^b - t)Cp_s/\Delta h]$

Superscripts

b	bulk solution
i	vapour-liquid interface
l	liquid
s	saturated or equilibrium
v	vapour
w	wall
$*$	dew point

Subscripts

$\bigcirc$	reference condition
avg	average
bot	absorber bottom
h	heat transfer
m	mass transfer
s	solution
sub	subcooling
top	absorber top
w	cooling water

system. [16–17] adopted a similar approach but used $\Delta T_{avg} = T^s(x^b_{top}, p) - t_{bot}$.

Similar to Eq. (1), mass flux at vapour-liquid interface can be written as

$$\dot{n} = \rho D\left(\frac{\partial x}{\partial y}\right)_{y=\delta} \equiv \rho\beta'\Delta x \tag{4}$$

where β' is a local mass transfer coefficient and Δx is the driving potential for mass transfer.

The average mass flux at vapour–liquid interface is expressed as

$$\dot{n}_{avg} \equiv \rho\beta\Delta x_{avg} \tag{5}$$

where β is an average mass transfer coefficient and Δx_{avg} is an average concentration difference most commonly defined as

$$\Delta x_{avg} \equiv \frac{\Delta x_{top} - \Delta x_{bot}}{\ln(\Delta x_{top}/\Delta x_{bot})} \tag{6}$$

For Δx in Eq. (6), $\Delta x = x^b - x^i$ was used in the isothermal absorption studies including [18,19] and also in many non-isothermal absorption studies including [5,8,11,12,17].

On the other hand, Kim et al. [20] used a rather unusual average driving force called "the logarithmic mean concentration difference of pressure difference" to take account of the non-condensable gas in vapour phase. [14] used $\Delta x_{avg} = (x^b - x^i)/x^i$ determined by the arithmetic averages of T^b and x^b. [15] used the difference between the bulk concentrations at the inlet and outlet, i.e. $\Delta x_{avg} = x^b_{top} - x^b_{bot}$, to avoid using the interface concentrations which they did not measure.

Except for the studies such as Yüksel and Schlünder [13] where interface concentration x^i has been determined from measured interface temperature, x^i has to be calculated somehow from the condition of bulk solution. In the isothermal absorption studies [18,19], it was calculated with Henry's law. And among the non-isothermal absorption studies above, [12] used the model of Yüksel and Schlünder [13], Kim and Infante Ferreira [8] used the method described in Appendix B, Hihara and Saito [5] and Yoon et al [11] assumed $x^i = x^s(T^b, p)$ and Bourouis et al. [17] did not clearly mention how they determined it.

As previously mentioned, a few recent studies have addressed this problem, namely Islam et al. [1–3] and Fujita and Hihara [4].

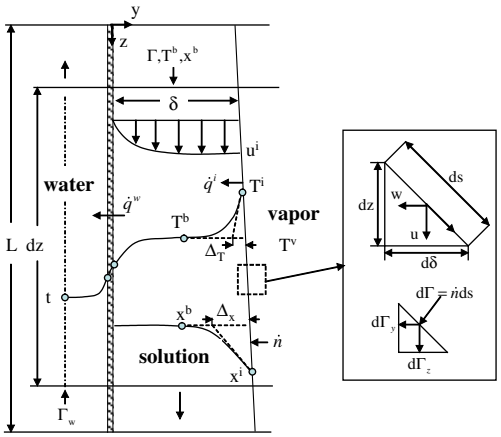

Fig. 1. Control volume element of a falling film absorber.

Islam et al. [1–3] derived two differential equations for heat and mass transfer from the governing equations of a counter-current falling film absorber and used the solution to determine experimental heat and mass transfer coefficients. Their approach was similar to what will be presented in the next section but the formulation of the governing equations in [1–3] was done in such a way that the physics in the absorption process was insufficiently accounted for.

Fujita and Hihara [4] showed the inadequateness of logarithmic mean potentials such as Eqs. (3) and (6) by comparing them with their analytic model. In their model, it was assumed that the driving potential for mass transfer into a falling film solution flow was proportional to the difference between the chemical potentials of bulk solution and vapour and set $\Delta x = ln(p)–ln[p^s(x^b,T^b)]$. However, their model had a few week points. First of all, chemical potential difference is a total driving force towards an equilibrium state and therefore it is a driving force not only for mass but also for heat transfer. Besides the chemical potential is proportional to $T \times ln(p)$ not to $ln(p)$. By neglecting the temperature term, they consequently assumed that the temperature at vapour–liquid interface was constant, which is only acceptable for isothermal absorption.

In the following, firstly, a new method is proposed for the determination of experimental heat and mass transfer coefficients based on the analytical solutions of the governing equations for falling film flows. Secondly, the new method is demonstrated by reprocessing the experimental data from [8,14].

2. Analytic modelling of falling film flows

Fig. 1 shows a control volume element in the falling film flow on a vertical wall, where vapour is absorbed at the vapour–liquid interface and heat is removed across the wall by the cooling water flowing on the other side.

In this study, the following has been assumed:

- Absorbent is not volatile.
- Fluid properties are constant.
- Heat and mass transfer coefficients are constant.

Justification of these two last assumptions will be given for the data used in the further analysis.

Mass and energy conservation for the control element give a total mass balance equation as

$$\frac{d\Gamma_s}{dz} = \dot{n}, \tag{7}$$

an absorbent mass balance equation as

$$\frac{d(\Gamma_s x^b)}{dz} = 0, \tag{8}$$

an energy balance equation as

$$\frac{d\left(\Gamma_s h^b\right)}{dz} = \dot{n}h^v - \dot{q}^w, \tag{9}$$

which can be approximated by (see Appendix A)

$$\frac{d\left(\Gamma_s Cp_s T^b\right)}{dz} = \dot{n}\Delta h - \dot{q}^w, \tag{10}$$

and finally an energy balance equation for the cooling water as

$$\frac{dt}{dz} = -\left(\frac{1}{\Gamma_w Cp_w}\right)\dot{q}^w \tag{11}$$

where a minus sign has been taken for counter-current flow configuration.

In Eqs. (7)–(11), wall heat flux $\dot{q}^w$ is defined between bulk solution and water temperatures by

$$\dot{q}^w = U(T^b - t) \tag{12}$$

and mass flux $\dot{n}$ is given by Eq. (B.14) in Appendix B assuming $\Phi_m = \Phi_h = 1$ as

$$\dot{n} = \rho\beta(c_1 T^b + c_2 x^b + c_3) \tag{13}$$

In order to solve the differential equation system, the number of variables is reduced as follows. Firstly, multiplying Eqs. (10), (8), and (7), respectively, with c_1/Cp_s, c_2 and c_3 and summing them up gives, after noting that from Eq. (13), $\dot{n}/\rho\beta = c_1 T^b + c_2 x^b + c_3$,

$$\frac{d}{dz}\left(\Gamma_s \frac{\dot{n}}{\rho\beta}\right) = \left[\dot{n}\left(\frac{c_1\Delta h}{Cp_s} + c_3\right) - \frac{c_1\dot{q}^w}{Cp_s}\right], \tag{14}$$

which in turn can be approximated by

$$\frac{d}{dz}\left(\frac{\dot{n}}{\rho\beta}\right) = \frac{1}{\Gamma_s}\left(\frac{c_1\Delta h}{Cp_s} + c_3\right)\dot{n} - \frac{c_1}{\Gamma_s Cp_s}\dot{q}^w \tag{15}$$

for $\Gamma_s \gg \int \dot{n}dz$ can be assumed that $\Gamma_s \approx \Gamma_{s,top}$.

Similarly, dividing Eq. (10) with $\Gamma_s Cp_s$ and subtracting Eq. (11) from it gives, after noting that, from Eq. (12), $\dot{q}^w/U = T^b - t$,

$$\frac{d}{dz}\left(\frac{\dot{q}^w}{U}\right) = \left(\frac{\Delta h}{\Gamma_s Cp_s}\right)\dot{n} - \left(\frac{1}{\Gamma_s Cp_s} - \frac{1}{\Gamma_w Cp_w}\right)\dot{q}^w \tag{16}$$

Eqs. (16) and (15) are made dimensionless as

$$\frac{d\omega}{d\zeta} = \bar{\beta}\phi - \overline{U}C\omega \tag{17}$$

$$\frac{d\phi}{d\zeta} = \bar{\beta}B\phi - \overline{U}(B - c_3)\omega \tag{18}$$

where $\omega = \dot{q}^w Cp_s/(U\Delta h)$, $\phi = \dot{n}/\rho\beta$, $\zeta = z/L$, $\bar{\beta} = \rho\beta L/\Gamma_s$, $\overline{U} = UL/(\Gamma_s Cp_s)$, $C = 1 - \Gamma_s Cp_s/(\Gamma_w Cp_w)$ and $B = c_1\Delta h/Cp_s + c_3$.

Eqs. (17) and (18) form an eigenvalue problem (see e.g. Ch. 4 in [21]), whose solution is given by

$$\begin{bmatrix}\phi\\ \omega\end{bmatrix} = -\left(\frac{\phi_{top} - v_2\omega_{top}}{v_2 - v_1}\right)\begin{bmatrix}v_1\\ 1\end{bmatrix}e^{\lambda_1\zeta} + \left(\frac{\phi_{top} - v_1\omega_{top}}{v_2 - v_1}\right)\begin{bmatrix}v_2\\ 1\end{bmatrix}e^{\lambda_2\zeta} \tag{19}$$

where eigenvector elements are given by

$$v_2,\ v_1 = \{B + C\overline{U}/\bar{\beta} \pm [(B - C\overline{U}/\bar{\beta})^2 + 4\overline{U}/\bar{\beta}(CB - B + c_3)]^{0.5}\}/2 \tag{20}$$

and the corresponding eigenvalues λ_1 and λ_2 are calculated by

$$\lambda = \bar{\beta}v - C\overline{U} \tag{21}$$

Eq. (19) would readily give heat and mass flux profiles, subsequently, if U and β were given, T^b and x^b profiles could be obtained from Eqs. (12) and (13). However, calculation of U and β back from ω and ϕ determined by experimental data is not so obvious. First of all, it is noted from Eqs. (19)–(21) that inlet and outlet conditions should satisfy

$$\ln\left(\frac{\phi_{bot} - v_2\omega_{bot}}{\phi_{top} - v_2\omega_{top}}\right) = \bar{\beta}\left[v_1 - C\left(\frac{\overline{U}}{\bar{\beta}}\right)\right] \tag{22}$$

$$\ln\left(\frac{\phi_{bot} - v_1\omega_{bot}}{\phi_{top} - v_1\omega_{top}}\right) = \bar{\beta}\left[v_2 - C\left(\frac{\overline{U}}{\bar{\beta}}\right)\right] \tag{23}$$

Removing $\bar{\beta}$ from Eqs. (22) and (23) leaves $\overline{U}/\bar{\beta}$ as a single unknown in

$$\left[v_2 - C\left(\frac{\overline{U}}{\bar{\beta}}\right)\right] \times \ln\left(\frac{\phi_{bot} - v_2\omega_{bot}}{\phi_{top} - v_2\omega_{top}}\right) = \left[v_1 - C\left(\frac{\overline{U}}{\bar{\beta}}\right)\right] \times \ln\left(\frac{\phi_{bot} - v_1\omega_{bot}}{\phi_{top} - v_1\omega_{top}}\right) \tag{24}$$

Since Eq. (24) is not convenient for solution, it is rearranged as

$$\phi_{bot} = v_2\omega_{bot} + (\phi_{top} - v_2\omega_{top}) \times \exp\left\{\left[\frac{v_1 - C(\overline{U}/\bar{\beta})}{v_2 - C(\overline{U}/\bar{\beta})}\right] \times \ln\left(\frac{\phi_{bot} - v_1\omega_{bot}}{\phi_{top} - v_1\omega_{top}}\right)\right\} \tag{25}$$

where the negative value from Eq. (20) should be chosen for v_1. Any numerical technique can be used to find a $\overline{U}/\bar{\beta}$ that brings the right-hand side of Eq. (25) close enough to a given ϕ_{bot} on the left. Inserting $\overline{U}/\bar{\beta}$ determined from Eq. (25) into either Eqs. (22), (23) gives $\bar{\beta}$ and thus $\overline{U}$.

It is noted that integration of Eqs. (17) and (18) from $\zeta = 0$ to 1 gives

$$\omega_{bot} = \omega_{top} + (L/\Gamma_s) \times \dot{n}_{avg} - CL/(\Gamma_s\Delta h) \times \dot{q}^w_{avg} \tag{26}$$

$$\phi_{bot} = \phi_{top} + (BL/\Gamma_s) \times \dot{n}_{avg} - (B - c_3)L/(\Gamma_s\Delta h) \times \dot{q}^w_{avg}, \tag{27}$$

which relate inlet and outlet conditions with average heat and mass fluxes. Since no heat and mass transfer coefficients are involved, Eqs. (26) and (27) can be used to check the consistency between experimental data and the present model.

For a quick analysis, one may assume constant heat and mass flux, respectively, in Eqs. (15) and (16) to obtain

$$U = \frac{\Gamma_s Cp_s}{CL} \times \ln\left[\frac{(T^b - t)_{top} - \dot{n}_{avg}\Delta h/(UC)}{(T^b - t)_{bot} - \dot{n}_{avg}\Delta h/(UC)}\right] \tag{28}$$

$$\beta = \frac{\Gamma_s}{\rho BL} \times \ln\left[\frac{(x^b - x^i)_{bot} - c_1\dot{q}^w_{avg}/(\rho\beta BCp_s)}{(x^b - x^i)_{top} - c_1\dot{q}^w_{avg}/(\rho\beta BCp_s)}\right] \tag{29}$$

Note that Eqs. (28) and (29) approach their counterparts in sensible heat transfer and the absorption of sparingly soluble gases (see e.g. [18,19]) when $\dot{n}_{avg}$ and $\dot{q}^w_{avg}$ approach zero. Again, Eqs. (28) and (29) are not readily solvable. Instead, the following rearrangements give fast-converging solutions.

$$U = \frac{\dot{n}_{avg}\Delta h}{C}\left[\frac{1 - \exp(UCL/\Gamma_s Cp_s)}{(T^b - t)_{top} - (T^b - t)_{bot}\exp(UCL/\Gamma_s Cp_s)}\right] \tag{30}$$

$$\beta = \frac{c_1\dot{q}^w_{avg}}{\rho BCp_s}\left[\frac{1 - \exp(\rho\beta BL/\Gamma_s)}{(x^b - x^i)_{bot} - (x^b - x^i)_{top}\exp(\rho\beta BL/\Gamma_s)}\right] \tag{31}$$

Starting with initial estimates from the right-hand sides, the resulting U and β on the left are fed back to the right sides and then the process is repeated until the changes become acceptably small.

It should be warned that Eqs. (28)–(31) are approximately valid only when heat and mass flux profiles do not change significantly along the absorber and therefore would give large errors when this condition is not met.

3. Application of the results

For demonstration of the results, the experimental data of Takamatsu et al. [14] and Kim and Infante Ferreira [8] have been reprocessed and the results are presented in the following.

First of all, several dimensionless numbers have been defined as follows.

In order to measure the uncertainties involved in the data processing, two error indices are defined by

$$(\Delta\omega/\omega)_{bot} \equiv [(T^b_{bot} - t_{bot})Cp_s/\Delta h - \omega_{bot}]/\omega_{bot} \tag{32}$$

$$(\Delta\phi/\phi)_{bot} \equiv [(c_1T^b_{bot} + c_2x^b_{bot} + c_3) - \phi_{bot}]/\phi_{bot}, \tag{33}$$

where T^b_{bot} and t_{bot} are the temperatures of bulk solution and cooling water measured at the absorber outlet and ω_{bot} and ϕ_{bot} are obtained from Eqs. (26) and (27) with $\omega_{top} = (T^b - t)_{top}Cp_s/\Delta h$ and $\phi_{top} = (c_1T^b_{top} + c_2x^b_{top} + c_3)$ determined from the experimental data. Eqs. (32) and (33) may be considered as the uncertainties in heat and mass transfer coefficients, respectively.

The Nusselt number has been defined as

$$Nu = \alpha^b/k \times (\nu^2/g)^{1/3} \tag{34}$$

where α^b is the film heat transfer coefficient between bulk solution and the wall which is calculated back from U.

The Sherwood number has been defined as

$$Sh = \beta/D \times (\nu^2/g)^{1/3} \tag{35}$$

Before presenting the results, it should be stated that the heat and mass transfer correction factors, i.e. Φ_m and Φ_h (see Appendix B), were neglected in the following analysis. It has thus been assumed that heat and mass are transferred only via diffusion at the interface.

3.1. Takamatsu et al. [14]

Takamatsu et al. [14] presented experimental data for the absorption of water vapour into falling film flows of 53 wt% aqueous LiBr solution inside of a 400-mm long copper tube with 19.05 mm diameter (internal diameter 16.05 mm) in the film Reynolds number range from 50 to 550. They compared their results with those of Kim and Kang [22] and pointed out that Nusselt and Sherwood numbers were strongly dependent on the subcooling of the inlet solution and on the tube length.

They calculated heat transfer coefficients using an arithmetic mean difference between bulk solution and wall temperatures, i.e. $\Delta T_{avg} = (T^b - T^w)_{avg}$, and mass transfer coefficients assuming $\Delta x_{avg} = [(x^b - x^i)/x^i]_{avg}$ with x^i determined in a way much similar to that of Yüksel and Schlünder [13].

Fig. 2 shows the two error indices defined by Eqs. (32) and (33) calculated for the experimental data.

Fig. 2a suggests that uncertainty in the heat transfer coefficients would be well within ±10%. On the other hand, Fig. 2b suggests that uncertainty would be larger for mass transfer coefficients.

Figs. 3 and 4 show the original and recalculated Nusselt and Sherwood numbers respectively for two different inlet subcooling values ($\Delta T_{sub} = 0$, 5 K) and film Reynolds numbers above 100.

In Figs. 3a and 4a, it appears indeed that Nusselt and Sherwood numbers are dependent on inlet subcooling. According to the results, inlet subcooling influences positively on Nusselt number

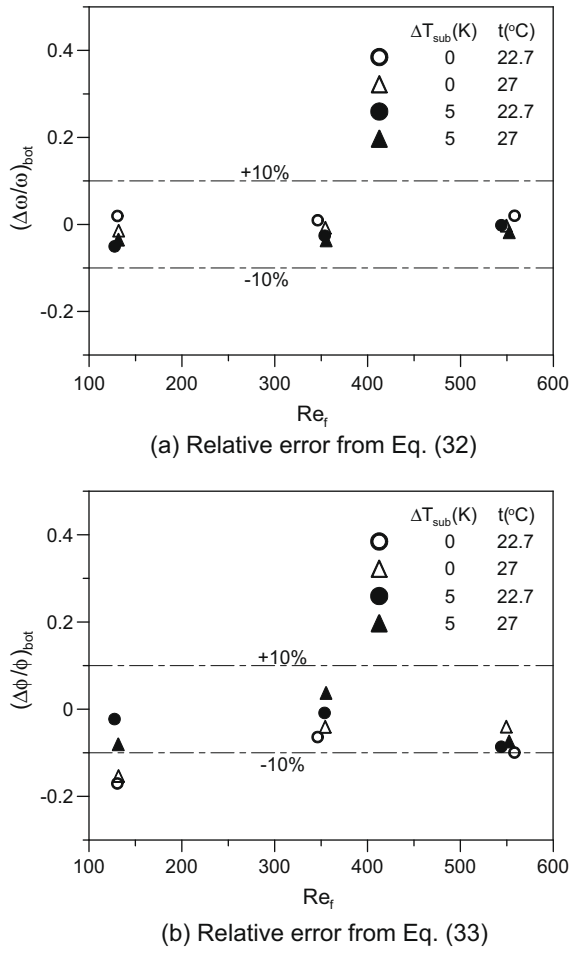

Fig. 2. Deviation of Takamatsu et al.'s [14] data from the analytic solution.

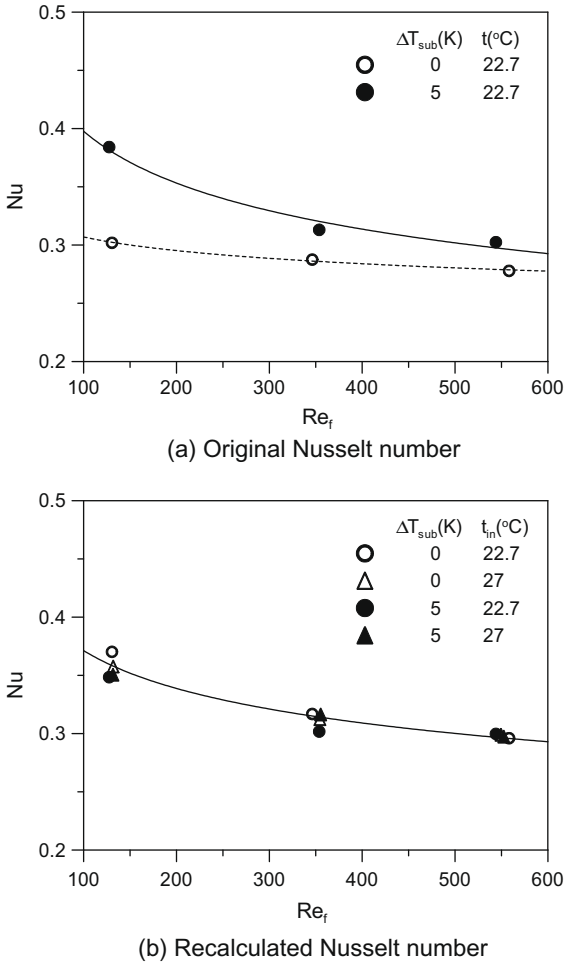

Fig. 3. Nusselt number comparison for Takamatsu et al. [14].

and negatively on Sherwood number, from which they reported that "the absorption process is largely dependent on the liquid subcooling at the inlet". Actually, the dependence of falling film flows' transfer coefficients on inlet conditions has also been reported by several other researchers including [10,22].

Figs. 3b and 4b show newly calculated Nusselt and Sherwood numbers, respectively, for the same experimental data according to the procedure explained in the previous section. Note that no systematic deviation can be found for different subcooling conditions. As expected, the consistency between the calculated transfer coefficients is very good for Nusselt numbers in Fig. 3b and it is reasonable for Sherwood numbers in Fig. 4b. Although it appears that the Sherwood numbers are somewhat dependent on cooling water temperature, it is not certain because the deviation is within the measurement errors reported in [14].

Although it cannot be concluded after a single set of data analysis that transfer coefficients are independent from inlet subcooling, the results in Figs. 3 and 4 suggest that there might be significant errors in those studies where transfer coefficients were reported to be dependent on inlet subcooling. Nevertheless the constant transfer coefficients that have been assumed in the present model must have introduced certain errors to the local temperature and concentration values and therefore contributed to the errors in Fig. 2.

Table 1 summarizes some of the properties used in the calculation. Variation of a property in the absorption processes is well within ±5% of its representative value. Therefore the assumption of constant properties is reasonable.

3.2. Kim and Infante Ferreira [8]

Kim and Infante Ferreira [8] reported experimental results for plate absorbers with different surface geometries and aqueous LiBr solutions (48–50wt%). Their absorber consisted of a copper plate heat exchanger with its $95 \times 540\ mm^2$ heat transfer surface exposed to an evacuated space within a 900-mm long ϕ150 mm glass tube. Solution was supplied through a liquid distributor at the top and collected by a receiver mounted at the bottom. They tested the heat exchanger with and without #22 copper-wire screen stretched over the heat transfer surface to measure its influence. They also measured the influence of octanol (2-ethyl-1-hexanol) as a surfactant.

They calculated heat transfer coefficients using Eq. (3) with $T = T^b$ and mass transfer coefficients using Eq. (6) with $\Delta x = x^b - x^i$ and x^i from Eq. (B.13) in Appendix B assuming $\Phi_m = \Phi_h = 1$.

Fig. 5 shows the two error indices for their experimental data.

Both error indices indicate that most of the data would agree with the new method with ±10% of uncertainty.

Fig. 6a and b show the original Nusselt numbers and newly calculated ones, respectively.

It is noted that while the difference is negligible for the cases without surfactant, it is substantial for the cases with surfactant. This suggests that error of the conventional method is large when heat and mass fluxes are large.

Fig. 7 shows newly calculated Sherwood numbers for the adiabatic and water-cooled test data. In [8], only the Sherwood numbers for adiabatic test results were presented because some of

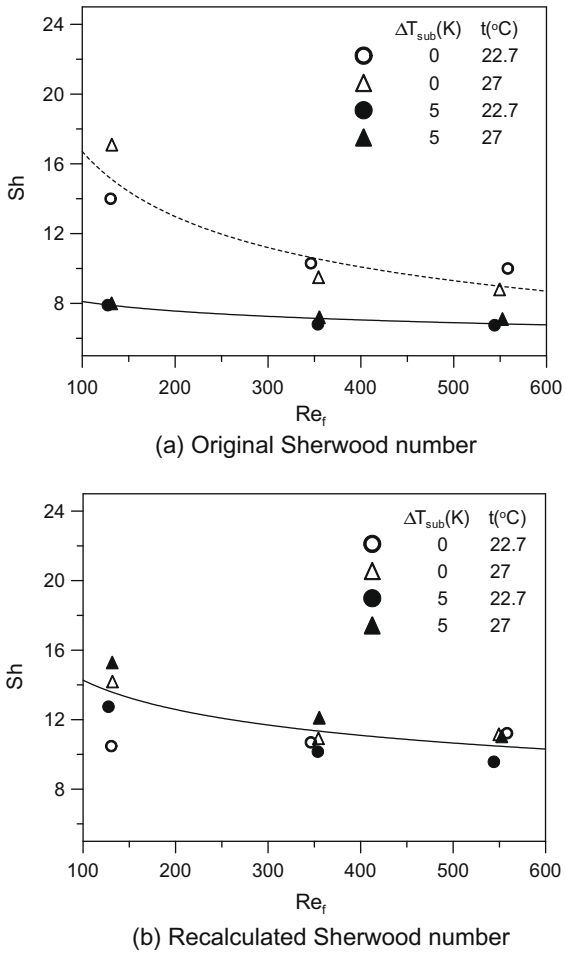

Fig. 4. Sherwood number comparison for Takamatsu et al. [14].

water-cooled tests were done with superheated solutions at the absorber inlet so that the logarithmic mean concentration difference could not be defined.

The newly calculated Sherwood numbers for the adiabatic test data are found only slightly different from the original ones suggesting that the conventional method was acceptable for the adiabatic data. Another interesting point from Fig. 7 is that Sherwood numbers are so much different for adiabatic and water-cooled data. Depending on the heat transfer surface and surfactant concentration, the Sherwood numbers have increased by 2–10 times when the absorber was cooled by cooling water implying that the wall heat flux significantly influenced the mass transfer process.

Table 2 summarizes some of the properties used in the calculation. Variation of a property in the absorption processes is within ±10% of its representative value. Therefore the error of constant property assumption is larger than for the case of Takamatsu et al. [14].

It is interesting to compare the data of Takamatsu et al. [14] and Kim and Infante Ferreira [8]. Figs. 3b and 6b exhibit different trends against film Reynolds number. While Nusselt number increases with decreasing film Reynolds number in Fig. 3b, it decreases in most cases of Fig. 6b. It should however be noticed that most experiments reported by [8] apply for relatively low Reynolds numbers for which complete wetting of the surface cannot be expected. This is the main reason for the different trends in Fig. 6b. The wet fraction of the heat transfer surface in [8] was observed to increase with film Reynolds number within the test range. This agrees with the observation of Takamatsu et al [14] that the surface was incompletely wet for the film Reynolds numbers below 130. On the other hand, Sherwood numbers in both studies show similar trends in Figs. 4b and 7b, where Sherwood numbers commonly increase with decreasing film Reynolds number. For the Sherwood number of Takamatsu et al. [14], this trend seems reasonable considering that Yüksel and Schlünder [13] also reported the same trend from their measurement in the corresponding film Reynolds range. But for Kim and Infante Ferreira [8], it may be prudent to postpone a conclusion due to the absence of comparable data in the literature.

4. Conclusions

Two differential equations have been derived from the governing equations of a falling film absorber by applying film theory and mixture thermodynamics, from which eigenvalue solutions were obtained for the temperature and concentration profiles. Based on these analytic solutions, a new method has been proposed for experimental determination of heat and mass transfer coefficients and its successful application has been demonstrated by reprocessing the experimental data of Takamatsu et al [14] and Kim and Infante Ferreira [8]. The reprocessed results of Takamatsu et al. [14] showed that the originally reported transfer coefficients' dependence on inlet conditions resulted from a misinterpretation of the experimental data due to the invalid definition of driving potentials. Reprocessing of Kim and Infante Ferreira [8]'s data revealed that the errors of conventional methods were substantial

Table 1
Properties used in the recalculation of experimental data from Takamatsu et al. [14].

Re_f	$\Delta T_{sub}/t_{in}$	x^b (in/out)	T^b (in/out)	[1] $\partial T^s/\partial x$	[2] $a \times 10^{+3}$	* Le	* Pr
130.5	0 K/22.7 °C	0.540/0.530	39.7/33.6	$181.4_{\pm 4.4}^{\pm 0}$	$1067_{\pm 3}^{\pm 0}$	71.9 ± 3.4	15.4 ± 0.4
346.2		0.536/0.533	38.9/34.2	$177.8_{\pm 1.2}^{\pm 0}$	$1067_{\pm 1}^{\pm 0}$	72.0 ± 3.1	15.4 ± 0.5
558.2		0.539/0.538	39.7/35.7	$180.4_{\pm 0.6}^{\pm 0}$	$1069_{\pm 0}^{\pm 0}$	71.0 ± 2.7	15.4 ± 0.5
131.8	0 K/27.0 °C	0.539/0.531	39.5/35.4	$180.6_{\pm 3.6}^{\pm 0}$	$1067_{\pm 3}^{\pm 0}$	70.8 ± 2.1	15.2 ± 0.2
354.4		0.538/0.536	39.4/35.8	$179.9_{\pm 0.9}^{\pm 0}$	$1068_{\pm 1}^{\pm 0}$	71.0 ± 2.3	15.3 ± 0.4
549.4		0.538/0.537	39.4/36.3	$179.9_{\pm 0.4}^{\pm 0}$	$1069_{\pm 0}^{\pm 0}$	70.8 ± 2.1	15.3 ± 0.4
127.5	5 K/22.7 °C	0.535/0.524	33.6/32.8	$176.8_{\pm 4.6}^{\pm 0}$	$1063_{\pm 3}^{\pm 0}$	76.1 ± 0.4	15.8 ± 0.4
353.7		0.535/0.531	33.8/33.5	$176.9_{\pm 1.5}^{\pm 0}$	$1066_{\pm 1}^{\pm 0}$	76.0 ± 0.1	16.1 ± 0.1
544.0		0.536/0.534	34.0/33.7	$177.8_{\pm 0.9}^{\pm 0}$	$1067_{\pm 1}^{\pm 0}$	76.1 ± 0.0	16.2 ± 0.1
131.6	5 K/27.0 °C	0.540/0.531	34.6/35.3	$180.9_{\pm 3.8}^{\pm 0}$	$1067_{\pm 3}^{\pm 0}$	74.5 ± 1.4	15.9 ± 0.6
355.3		0.537/0.534	34.2/35.2	$178.8_{\pm 1.4}^{\pm 0}$	$1067_{\pm 1}^{\pm 0}$	74.9 ± 1.1	16.0 ± 0.3
552.5		0.536/0.534	34.2/35.0	$177.4_{\pm 0.8}^{\pm 0}$	$1067_{\pm 1}^{\pm 0}$	74.9 ± 0.8	15.9 ± 0.2

[1,2] Calculated from the inlet bulk conditions.
* Calculated with the average bulk conditions. Differences from the inlet and outlet properties are denoted by ±sign.

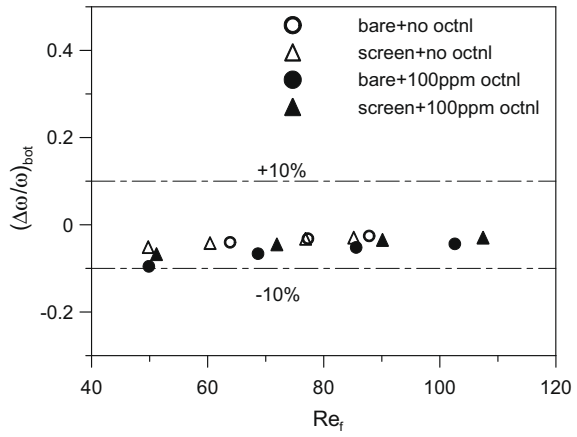

(a) Relative error from Eq. (32)

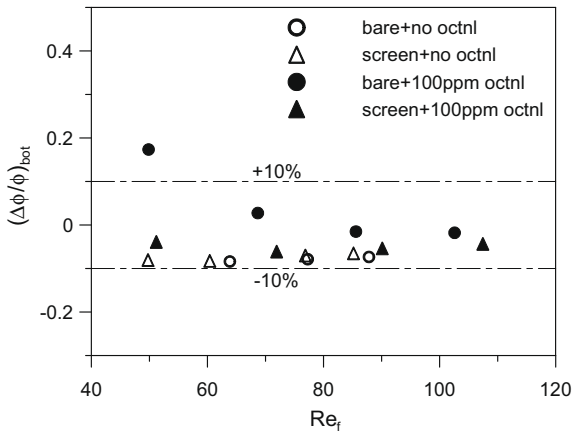

(b) Relative error from Eq. (33)

Fig. 5. Deviation of Kim and Infante Ferreira [8]'s data from the analytic solution.

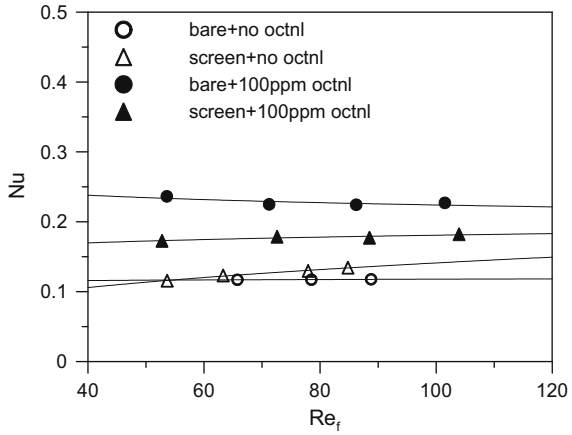

(a) Original Nusselt number

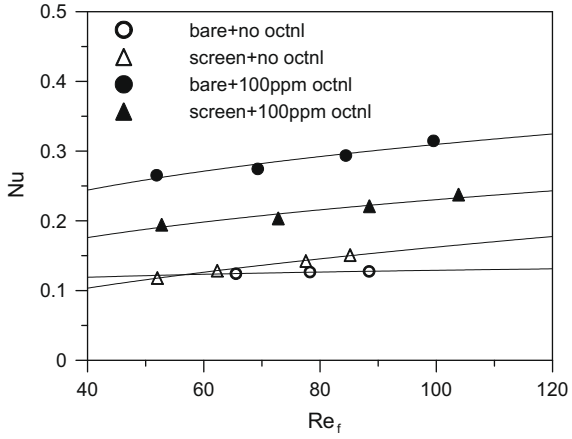

(b) Recalculated Nusselt number

Fig. 6. Nusselt number comparison for Kim and Infante Ferreira [8].

when heat and mass fluxes were large and the mass transfer in falling film flows was significantly promoted by the intensity of wall heat flux.

Appendix A. Solution thermodynamics in sorption processes

The energy balance over a control volume element in an absorbing or desorbing falling film flow is given by

$$\frac{d(\Gamma_s h^b)}{dz} = \dot{n}h^v - \dot{q}^w \tag{A.1}$$

Haltenburger [23] showed that for isothermal evaporation from a solution, the solution enthalpy at concentration x could be calculated from a reference concentration x_o by

$$h^{l,s} = \frac{x}{x_o}h_o^{l,s} + x\int_{x_o}^{x}\bar{h}d\left(\frac{1}{x}\right) \tag{A.2}$$

where $\bar{h}$ is the partial specific enthalpy of the refrigerant in the solution. For low-pressure systems, $\bar{h}$ can be approximated by

$$\bar{h} = h^{v,s} - \Delta h \tag{A.3}$$

where $\Delta h \equiv ah^{fg}$ and a is defined by

$$a = \left(\frac{T}{T^*}\right)^2\frac{dT^*}{dT} \tag{A.4}$$

which is the slope of the $1/T^*-1/T$ curve for the solution with a fixed concentration.

Since the bulk solution is not saturated, h^b in Eq. (A.1) can be written as

$$h^b = \frac{x}{x_o}h_o^{l,s} + x\int_{x_o}^{x}\bar{h}d\left(\frac{1}{x}\right) + Cp_s(T^b - T_o^s) \tag{A.5}$$

where T_o^s is the saturation temperature of the reference solution at the given pressure, i.e. $T_o^s = T^s(x_o, p)$.

Multiplying Γ_s with Eq. (A.5) and differentiating gives

$$\frac{d(\Gamma_s h^b)}{dz} = \dot{n}(\bar{h} - Cp_s T_o^s) + \frac{d}{dz}(\Gamma_s Cp_s T^b) \tag{A.6}$$

Inserting Eq. (A.6) into Eq. (A.1) and rearranging it gives

$$\frac{d}{dz}(\Gamma_s Cp_s T^b) = \dot{n}\left[\Delta h + Cp_s T_o^s - Cp^v(T^s - T^v)\right] - \dot{q}^w \tag{A.7}$$

where the sensible term $Cp_s T_o^s - Cp^v(T^s - T^v)$ in the bracket on the right-hand side is normally negligibly small in comparison with Δh and may be neglected.

Appendix B. Heat and mass transfer at vapour–liquid interface

Film theory, see e.g. [24,25], postulates that mass is transferred from the interface to the bulk flow through a thin hypothetical stagnant layer where convection is neglected in flow direction. The concentration profile in this layer is distorted by the mass con-

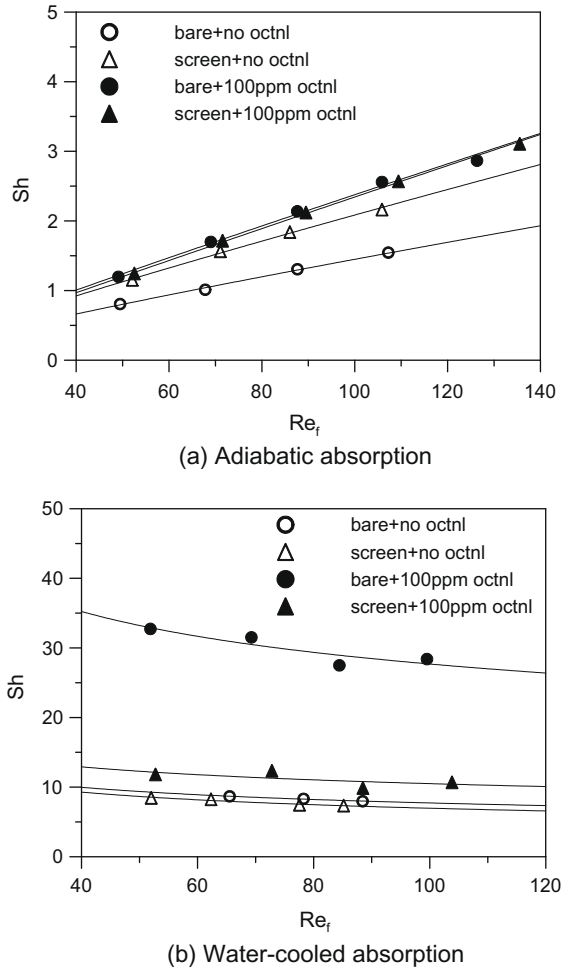

Fig. 7. Recalculated Sherwood numbers for Kim and Infante Ferreira [8].

vection in transverse direction, which can be substantially different from that of pure diffusion.

According to the film theory, the mass flux at the vapour-liquid interface $\dot{n}$ can be expressed as

$$\dot{n} = \Phi_m \rho \beta (x^b - x^i) \tag{B.1}$$

where mass transfer coefficient β is defined by $\beta \equiv D/\Delta_x$. Φ_m is a correction factor for the unidirectional mass transfer across the boundary layer Δ_x in Fig. 1, which is defined by

$$\Phi_m = \frac{1}{x^i}\left(\frac{\phi}{e^\phi - 1}\right) \tag{B.2}$$

where $\phi \equiv \dot{n}/(\rho\beta) = 1/St_m$. In Eq. (B.2), Φ_m approaches 1.0 when $\phi \to 0$ and $x^i \to 1$.

Eq. (B.2) assumes, however, that the whole mass absorbed at the interface is transferred by convection into the film. But this assumption is disputable for falling film absorption, where convective mass transfer can be small in transverse direction.

For example, considering the triangular element at the interface in Fig. 1, mass balance equation is given by

$$d\Gamma_y = d\Gamma - \rho u^i d\delta \tag{B.3}$$

where a uniform velocity u^i has been assumed along $d\delta$ and the film thickness δ is given for laminar falling film flows as

$$\delta = c(\nu^2/g)^{1/3} Re_f^b \tag{B.4}$$

with c and b being constants.

From Eq. (B.4) and $Re_f \equiv 4\Gamma_s/\mu (= 4\rho u_{avg}\delta/\mu)$, Eq. (B.3) gives the ratio of the transversal convection to the total absorption rate as

$$\frac{d\Gamma_y}{d\Gamma} = 1 - b\left(\frac{u^i}{u_{avg}}\right) \tag{B.5}$$

which can be substantially smaller than 1.0 as Nusselt [26] gives $d\Gamma_y/d\Gamma = 0.5$ with $b = 1/3$ and $u^i/u_{avg} = 1.5$ for laminar film flows.

Therefore, when applied to falling film flows, Eq. (B.2) may be modified as

$$\Phi_m = \frac{F}{x^i}\left(\frac{\phi}{e^\phi - 1}\right) \tag{B.6}$$

where F ($\leqslant 1$) is a newly introduced modification factor.

Similar to Eq. (B.1), the heat flux $\dot{q}^i$ from the interface to bulk solution is given by

$$\dot{q}^i = \Phi_h \alpha^i (T^i - T^b) \tag{B.7}$$

where the heat transfer coefficient α^i is defined by $\alpha^i \equiv k/\Delta_T$. Φ_h is known as Ackermann's correction factor [24] for the convection effect across the boundary layer Δ_T in Fig. 1, which is defined similar to Eq. (B.6) by

Table 2
Properties used in the recalculation of water-cooled data from Kim and Infante Ferreira [8].

Re_f	Surface/Octnl	x^b (in/out)	T^b (in/out)	[1]$\partial T^s/\partial x$	[2]$a \times 10^{+3}$	*Le	*Pr
55.5	Bare/0 ppm	0.492/0.470	27.0/22.7	$138.1_{\pm 8.7}^{0}$	$1038_{\pm 5}^{0}$	83.2 ± 2.9	13.9 ± 0.2
65.5		0.491/0.474	27.3/22.9	$137.3_{\pm 6.8}^{0}$	$1039_{\pm 4}^{0}$	83.0 ± 3.2	14.0 ± 0.0
78.3		0.491/0.477	27.5/23.0	$137.2_{\pm 5.6}^{0}$	$1040_{\pm 3}^{0}$	82.9 ± 3.4	14.1 ± 0.1
88.4		0.491/0.479	27.3/23.0	$137.1_{\pm 4.9}^{0}$	$1040_{\pm 3}^{0}$	83.1 ± 3.3	14.2 ± 0.2
52.0	Screen/0 ppm	0.490/0.469	26.2/22.4	$136.3_{\pm 8.0}^{0}$	$1038_{\pm 4}^{0}$	84.1 ± 2.6	14.0 ± 0.2
62.3		0.490/0.473	26.2/22.4	$136.7_{\pm 6.8}^{0}$	$1039_{\pm 4}^{0}$	84.3 ± 2.7	14.2 ± 0.1
77.6		0.490/0.476	26.5/21.9	$135.9_{\pm 5.3}^{0}$	$1039_{\pm 3}^{0}$	84.7 ± 3.5	14.3 ± 0.2
85.2		0.489/0.477	26.7/21.7	$135.6_{\pm 4.8}^{0}$	$1039_{\pm 3}^{0}$	84.6 ± 4.0	14.3 ± 0.3
51.9	Bare/100 ppm	0.490/0.462	25.6/18.4	$134.6_{\pm 10.6}^{0}$	$1037_{\pm 6}^{0}$	88.2 ± 5.7	14.5 ± 0.0
69.3		0.490/0.470	26.5/19.0	$134.7_{\pm 7.9}^{0}$	$1038_{\pm 4}^{0}$	87.1 ± 6.1	14.5 ± 0.3
84.4		0.490/0.474	26.9/18.9	$134.3_{\pm 6.3}^{0}$	$1039_{\pm 3}^{0}$	87.0 ± 6.8	14.6 ± 0.8
99.5		0.490/0.477	27.3/18.8	$133.8_{\pm 5.1}^{0}$	$1040_{\pm 3}^{0}$	86.9 ± 7.4	14.7 ± 0.8
52.8	Screen/100 ppm	0.491/0.468	26.0/19.6	$136.3_{\pm 9.1}^{0}$	$1038_{\pm 5}^{0}$	86.8 ± 5.0	14.4 ± 0.1
72.8		0.490/0.473	25.5/19.9	$135.1_{\pm 6.7}^{0}$	$1039_{\pm 4}^{0}$	87.3 ± 4.6	14.6 ± 0.2
88.5		0.490/0.478	26.9/19.7	$135.4_{\pm 5.0}^{0}$	$1040_{\pm 3}^{0}$	86.4 ± 6.1	14.7 ± 0.6
103.8		0.490/0.479	26.9/19.2	$134.2_{\pm 4.0}^{0}$	$1040_{\pm 2}^{0}$	87.0 ± 6.8	14.8 ± 0.8

[1,2] Calculated from the inlet bulk conditions.
* Calculated with the average bulk conditions. Differences from the inlet and outlet properties are denoted by ±sign.

$$\Phi_h = \frac{F\varphi}{e^{F\varphi} - 1} \tag{B.8}$$

where $\varphi \equiv \dot{n} Cp_w/\alpha^i = 1/St_h$.

The energy balance at the interface is given by

$$\dot{q}^i = \dot{n}\Delta h \tag{B.9}$$

and the heat and mass transfer analogy relates the heat and mass transfer coefficients as

$$\alpha^i/\beta = \rho Cp_s Le^n \tag{B.10}$$

Noting Eq. (B.10), inserting Eqs. (B.1) and (B.7) into Eq. (B.9) and rearranging gives

$$x^b - x^i = (Cp_s Le^n/\Delta h)(\Phi_h/\Phi_m) \times (T^i - T^b) \tag{B.11}$$

which binds bulk and interface conditions so that energy and mass balances are satisfied at the interface.

Note that Eq. (B.11) approaches that of Nakoryakov and Grigoreva [27] when $\Phi_m = \Phi_h = 1.0$ and that of Yüksel and Shlünder [13] when $F = 1.0$ in Eqs. (B.6) and (B.8). For the exponent of Lewis number, $n = 0.5$ is given by [27] and $0.5 \leqslant n \leqslant 0.6$ by [13].

Since the solution at vapour–liquid interface can be assumed to be in equilibrium under the system pressure, expanding an equilibrium equation for aqueous LiBr solution in Taylor series and taking only the first two terms gives T^i as

$$T^i = \left(\frac{\partial T^s}{\partial x}\right)(x^i - x_o) + T^s_o \tag{B.12}$$

where x_o is the concentration of a reference solution, T^s_o is its equilibrium temperature, i.e. $T^s_o = T^s(x_o, p)$, and the gradient is defined by $(\partial T^s/\partial x) = \lim_{\Delta x \to 0}(\Delta T^s/\Delta x)$ at $x = x_o$.

Inserting Eq. (B.12) into Eq. (B.11) gives

$$x^b - x^i = c_1 T^b + c_2 x^b + c_3 \tag{B.13}$$

where $c_1 \equiv -1/[(\partial T^s/\partial x) + (\Phi_m/\Phi_h)\Delta h/(Cp_s \mathrm{Le}^n)]$, $c_2 \equiv -c_1(\partial T^s/\partial x)$ and $c_3 \equiv -c_1[T^s_o - (\partial T^s/\partial x)x_o]$.

Finally, inserting Eq. (B.13) into Eq. (B.1) gives

$$\dot{n} = \Phi_m \rho \beta (c_1 T^b + c_2 x^b + c_3) \tag{B.14}$$

References

[1] M.R. Islam, N.E. Wijeysundera, J.C. Ho, Evaluation of heat and mass transfer coefficients for falling-films on tubular absorbers, Int. J. Refrig. 26 (2003) 197–204.

[2] M.R. Islam, N.E. Wijeysundera, J.C. Ho, Simplified models for coupled heat and mass transfer in falling-film absorbers, Int. J. Heat Mass Transfer 47 (2004) 395–406.

[3] M.R. Islam, N.E. Wijeysundera, J.C. Ho, Heat and mass transfer effectiveness and correlations for counter-flow absorbers, Int. J. Heat Mass Transfer 49 (2006) 4171–4182.

[4] I. Fujita, E. Hihara, Heat and mass transfer coefficients of falling-film absorption process, Int. J. Heat Mass Transfer 48 (2005) 2779–2786.

[5] E. Hihara, T. Saito, Effect of surfactant on falling film absorption, Int. J. Refrig. 16 (1993) 339–346.

[6] C.W. Park, S.S. Kim, H.C. Cho, Y.T. Kang, Experimental correlation of falling film absorption heat transfer on micro-scale hatched tubes, Int. J. Refrig. 26 (2003) 758–763.

[7] K. Kwon, S. Jeong, Effect of vapor flow on the falling-film heat transfer of a helical coil, in: Proc. of Int. Congress of Refrig., Washington, DC, USA, 2003.

[8] D.S. Kim, C.A. Infante Ferreira, Effect of surface geometry and surfactants on the performance of falling films, in: Proc. 7th Gustav–Lorentzen Conference on Natural Working Fluids, Trondheim, Norway, 2006.

[9] L. Hoffmann, I. Greiter, A. Wagner, V. Weiss, G. Alefeld, Experimental investigation of heat and mass transfer in a horizontal-tube falling-film absorber with aqueous solutions of LiBr with and without surfactants, Int. J. Refrig. 19 (1996) 331–341.

[10] I.S. Kyung, K.E. Herold, Performance of horizontal smooth tube absorber with and without 2-ethyl-hexanol, J. Heat Transfer, Trans. ASME 124 (2002) 177–183.

[11] J.I. Yoon, E. Kim, K.H. Choi, W.S. Seol, Heat transfer enhancement with a surfactant on horizontal bundle tubes of an absorber, Int. J. Heat Mass Transfer 45 (2002) 735–741.

[12] Y.M. Chen, C.Y. Sun, Experimental study on the heat and mass transfer of a combined absorber–evaporator exchanger, Int. J. Heat Mass Transfer 40 (1997) 961–971.

[13] M.L. Yüksel, E.U. Schlünder, Heat and mass transfer in non-isothermal absorption of gases in falling liquid films part I: experimental determination of heat and mass transfer coefficients, Chem. Eng. Process 22 (1987) 193–202.

[14] H. Takamatsu, H. Yamashiro, N. Takata, H. Honda, Vapor absorption by LiBr aqueous solution in vertical smooth tubes, Int. J. Refrig. 26 (2003) 659–666.

[15] W.A. Miller, M. Keyhani, The correlation of simultaneous heat and mass transfer experimental data for aqueous lithium bromide vertical falling film absorption, J. Solar Energy Eng. 123 (2001) 30–42.

[16] M. Medrano, M. Bourouis, A. Coronas, Absorption of water vapor in the falling film of water–lithium bromide inside a vertical tube at air-cooling thermal conditions, Int. J. Thermal Sci. 41 (2002) 891–898.

[17] M. Bourouis, M. Vallès, M. Medrano, A. Coronas, Absorption of water vapor in the falling film of water–(LiBr + LiI + $LiNO_3$ + LiCl) in a vertical tube at air-cooling thermal conditions, Int. J. Thermal Sci. 44 (2005) 491–498.

[18] A.P. Lamourelle, O.C. Sandall, Gas absorption into a turbulent liquid, Chem. Eng. Sci. 27 (1972) 1035–1043.

[19] S.M. Yih, K.Y. Chen, Gas absorption into wavy and turbulent falling liquid films in a wetted-wall column, Chem. Eng. Commun. 17 (1982) 123–136.

[20] K.J. Kim, N.S. Berman, D.S.C. Chau, B.D. Wood, Absorption of water vapor into aqueous lithium–bromide, Int. J. Refrig. 18 (1995) 486–494.

[21] E. Kreyszig, Advanced Engineering Mathematics, seventh ed., John Wiley & Sons, New York, 1992.

[22] B.J. Kim, I.S. Kang, Absorption of water–vapor into wavy-laminar falling film of aqueous lithium bromide, KSME Int. J. 9 (1995) 115–122.

[23] W. Haltenburger Jr., Enthalpy–concentration charts from vapor pressure data, Ind. Eng. Chem. 31 (1939) 783–786.

[24] R.B. Bird, W.E. Stewart, E.N. Lightfoot, Transport Phenomena, Wiley, New York, 1965.

[25] H.D. Baehr, K. Stephan, Wärme- und Stoffübertragung, third ed., Springer-Verlag, Berlin, 1998.

[26] W. Nusselt, Die Oberflächenkondensation des Wasserdampfes, VDI Z. 60 (1916) 541.

[27] V.E. Nakoryakov, N.I. Grigoreva, Calculation of heat and mass transfer in nonisothermal absorption on the initial portion of a downflowing film, translated from Teoreticheskie Osnovy Khimicheskoi Tekhnologii 14 (1980) 483–488.